JOURNAL OF AIRCRAFT
Vol. 33, No. 5, September–October 1996

Higher-Order Shear Deformation Theory for Thin-Walled Composite Beams

J. K. Suresh* and V. T. Nagaraj†
Hindustan Aeronautics Limited, Bangalore 560 017, India

A higher-order shear deformation theory for the static and dynamic analysis of thin-walled composite beams of arbitrary lay-ups and cross sections is presented. The method is applicable to beams of open as well as closed cross sections. The formulation includes Euler–Bernoulli and Timoshenko theories as subsets. The bending- and torsion-related warping functions are derived in closed form. The method is validated by comparison with experimental and analytical results for static deflections of composite beams with symmetric and antisymmetric lay-ups. Comparison with experimental results for the vibration of beams exhibiting bending–torsion coupling shows that the present method gives better correlations. The significance of the higher-order theory is brought out by validating the results of the analyses against results from other theoretical methods. The results show the importance of the lay-up sequence on the shear lag in thin-walled composite beams.

Nomenclature

A_i	= area enclosed by walls of the beam cross section
A_{ij}	= membrane stiffness, Eq. (5)
A_{nn}, A_{ns}, A_{ss}	= membrane stiffnesses, Eq. (8)
$a_1(s) \ldots a_6(s)$	= contour warping functions, Eqs. (12), (14), and (23)
b	= width of the beam cross section
F	= generalized forces Eq. (32)
F_y, F_z, F_ϕ	= auxiliary functions, Eq. (24)
h	= depth of beam cross section
I_y	= area moment of inertia of cross section
K	= Timoshenko shear coefficient
$[K]$	= stiffness matrix, Eq. (33)
L	= length of beam
N_{xx}, N_{xs}, N_{ss}	= membrane stress resultants, Eq. (4)
P	= tip load
$\bar{Q}_{ij}$	= plane stress stiffnesses
q	= general coordinates, Eq. (31)
r	= radius vector, from the pole, to the midsurface of wall, Eq. (3)
S_y^*, S_z^*	= auxiliary functions, Eq. (17)
s	= contour coordinate
u, v, w, ϕ	= axial and lateral deflections, and twist
x, y, z	= beam coordinates
α	= cross-sectional constant of Eq. (30)
α_1, α_2	= parameters for optimization, Eq. (19)
β	= cross-sectional constant, Eq. (29)
β_y, β_z	= slopes of reference axes
ε_{xx}, ε_{ss}, γ_{xs}	= axial, hoop, and shear strains

I. Introduction

ADVANCED composite materials offer the benefits of lightweight structures that have good fatigue and damage tolerant behavior. Thin-walled box beam constructions have been used for primary components like helicopter rotor blades and wing spars. Composite materials offer the possibility of aeroelastic tailoring by introducing certain couplings, e.g., between bending and torsion or between axial elongation and torsion. To exploit these properties during the design phase it is advantageous to develop an analytical tool that reflects the special characteristics of composite materials. Such a model is also useful in understanding the various couplings.

There exist a number of theories for the analysis of isotropic thin walled beams with open or closed cross sections. In addition to the widely used Euler–Bernoulli theory, the influence of restrained torsional warping and shear deformation are considered.[1–5] A systematic, variationally consistent higher-order shear deformation theory for isotropic beams has been proposed by Krishna Murty[5] as an extension of his earlier work.[6,7] This method is capable of generating a hierarchy of models starting from the Euler–Bernoulli theory and progressing successively to the Timoshenko theory and then to the second and higher-order shear deformation theories.

The development of analytical tools for composite beams has resulted in a number of finite element based methods[8–10] and also direct analytical methods.[11–25] These methods have been surveyed.[26] While the finite element methods (FEMs) are powerful tools, they rely on comparatively larger computations and do not give the same amount of physical insight as the simpler, more direct methods.

Among the direct analytical methods, the pioneering work of Mansfield and Sobey[17] extended the classical Bredt–Batho analysis to composite thin-walled beams and recognized the potential for aeroelastic tailoring. Libove[18] developed a similar analysis and gave a more rigorous derivation of the equations.

Rehfield[19] proposed a model that included the effects of shear deformation in a manner similar to the Timoshenko theory. This was further elaborated by Rehfield et al.[21] where the influences of elastic bending-shear coupling and restrained warping were clearly brought out. The model of Smith and Chopra[22] is similar to Rehfield's model except in the treatment of the constitutive relations and torsion-related warping. More recently, Chandra and Chopra[25] have refined the torsion-related warping representation, which takes account of the variation of properties along the contour.

Rand[23,24] used a detailed description of both torsion- and shear-related warping effects in his analysis of thin-walled beams and has brought out the factors that give rise to structural couplings.

The direct analytical methods developed so far have been specialized either to open cross-sectional beams or to beams with one or two-cell cross sections. A correlation study shows that for composite beams exhibiting extension–torsion cou-

Received May 25, 1994; revision received April 1, 1996; accepted for publication April 29, 1996.

*Manager, Helicopter Design Bureau.
†Additional General Manager, Helicopter Design Bureau.

plings, the methods of Mansfield,[17] Rehfield,[19,21] and Smith and Chopra[22] give excellent correlations with both finite element[9] and experimental[20,27] results. However, for the composite beams exhibiting bending–torsion couplings, only Mansfield's method gives good correlations with experiment. Using the framework of Rehfield's theory,[19,21] it is shown in this article that it is possible to improve the correlations by proper representation of the torsion-related warping. A method for systematically deriving the warping functions for both shear and torsion is presented.

II. Outline of the Theory

A brief outline of Rehfield's method, which is the basis for the present method, is first presented. Consider a thin-walled beam whose x coordinate runs along a reference axis and the circumferential coordinate s runs along the midsurface of the walls. The beam undergoes the following generalized displacements: axial u, flatwise bending w, edgewise bending v, and twisting ϕ.

The displacement field is given by

$$\begin{aligned} u &= u(x, s) + y\beta_z(x) + z\beta_y(x) \\ v &= V(x) - z\phi(x) \\ w &= W(x) + y\phi(z) \end{aligned} \tag{1}$$

The corresponding strains on the midsurface of the wall of the cross section are

$$\varepsilon_{xx} = u_{,x} + y\beta_{z,x} + z\beta_{y,x} \tag{2}$$

$$\gamma_{xs} = u_{,s} + [V_{,x} + \beta_z]y_{,s} + [W_{,x} + \beta_y]z_{,s} + \boldsymbol{r}\phi_{,x} \tag{3}$$

where $\boldsymbol{r} = yz_{,s} - zy_{,s}$.

The variables β_z and β_y represent the slopes of the reference axis caused by bending, whereas $[V_{,x} + \beta_z]$ and $[W_{,x} + \beta_y]$ represent the slopes caused by shear deformation. For thin-walled beams, the local shell bending and twisting moment resultants can be ignored and only the membrane stress resultants N_{xx}, N_{xs}, and N_{ss} need to be considered. These are related to the membrane strains by

$$\begin{Bmatrix} N_{xx} \\ N_{ss} \\ N_{xs} \end{Bmatrix} = \begin{bmatrix} A_{11} & A_{12} & A_{16} \\ A_{12} & A_{22} & A_{26} \\ A_{16} & A_{26} & A_{66} \end{bmatrix} \begin{Bmatrix} \varepsilon_{xx} \\ \varepsilon_{ss} \\ \gamma_{xs} \end{Bmatrix} \tag{4}$$

where, for a laminate of N plies, the A_{ij} are determined from

$$A_{ij} = \sum_{k=1}^{N} \bar{Q}_{ij}^{(k)} h_k \qquad (i, j = 1, 2, 6) \tag{5}$$

where h_k is the thickness of the kth ply and $\bar{Q}_{ij}^{(k)}$ are the plane stress stiffnesses.

For closed cross sections, assuming that there is no internal pressure, the local shell bending and twisting moment can be ignored and we can set

$$N_{ss} = 0 \tag{6}$$

The hoop strain ε_{ss} can be eliminated from Eq. (4) to give

$$\begin{Bmatrix} N_{xx} \\ N_{xs} \end{Bmatrix} = \begin{bmatrix} A_{nn} & A_{ns} \\ A_{ns} & A_{ss} \end{bmatrix} \begin{Bmatrix} \varepsilon_{xx} \\ \gamma_{xs} \end{Bmatrix} \tag{7}$$

where

$$\begin{aligned} A_{nn} &= A_{11} - A_{12}^2/A_{22}; \qquad A_{xs} = A_{16} - A_{12}A_{26}/A_{22} \\ A_{ss} &= A_{66} - A_{26}^2/A_{22} \end{aligned} \tag{8}$$

III. Derivation of Warping Functions

The equilibrium of an element of the wall of the beam requires that

$$(N_{xs})_{,x} = 0, \quad \text{and} \quad (N_{xx})_{,x} + (N_{xs})_{,s} = 0 \tag{9}$$

When A_{nn} and A_{ss} are independent of x, the first of Eq. (9) implies that

$$(\gamma_{xs})_{,x} = -(A_{ns}/A_{ss})\varepsilon_{xx,x} \tag{10}$$

and the second of Eq. (9) gives

$$N_{xs} = N_{zs}^0 - \int_0^s [A_{nn} - A_{nn}^2/A_{ss}]\varepsilon_{xx,x}\, ds \tag{11}$$

where N_{xs}^0 is a constant in the cell and represents the statically indeterminate part of the shear flow.

From Eq. (7), the shear strain is given by

$$\gamma_{xs} = N_{xs}/A_{ss} - (A_{ns}/A_{ss})\varepsilon_{xx} \tag{12}$$

From Eqs. (11) and (12)

$$\gamma_{xs} = \frac{N_{zs}^0}{A_{ss}} - \frac{1}{A_{ss}} \int_0^s \left[A_{nn} - \frac{A_{nn}^2}{A_{ss}}\right] \varepsilon_{xx,x}\, ds - \frac{A_{ns}}{A_{ss}}\, \varepsilon_{xx} \tag{13}$$

From kinematical considerations, γ_{xs} is also given by Eq. (2). Continuity of the axial displacement requires that

$$\oint u_{,s}\, ds = 0 \tag{14}$$

Equations (2), (13), and (14) define N_{xs}^0 and also the warping functions. Neglecting the last term in Eq. (13), an approximation to the axial deformation can be expressed in the form

$$u = u_1 + y\beta_z + z\beta_y - a_3(s)\phi_{,x} - a_4(s)\psi_v - a_5(s)\psi_w \tag{15}$$

where

$$\begin{aligned} a_3(s) &= \int_0^s [(F_\phi/A_{ss}) - \boldsymbol{r}]\, ds \\ a_4(s) &= \int_0^s [(F_y - S_y^*)/A_{ss}]\, ds \\ a_5(s) &= \int_0^s [(F_z - S_z^*)/A_{ss}]\, ds \\ F_\phi &= \oint r \frac{ds}{\oint \left(\frac{ds}{A_{ss}}\right)} = 2A_1 \Big/ \oint \left(\frac{ds}{A_{ss}}\right) \\ S_y^* &= \int_0^s \left[A_{nn} - \left(\frac{A_{ns}^2}{A_{ss}}\right)\right] y\, ds \\ S_z^* &= \int_0^s \left[A_{nn} - \left(\frac{A_{ns}^2}{A_{ss}}\right)\right] z\, ds \\ F_y &= \oint \left[\frac{S_y^*}{A_{ss}}\right] ds \Big/ \oint \left(\frac{ds}{A_{ss}}\right) \\ F_z &= \oint \left[\frac{S_z^*}{A_{ss}}\right] \frac{ds}{\oint \left(\frac{ds}{A_{ss}}\right)} \end{aligned} \tag{16, 17}$$

and A_1 is the area of the cross section of the cell.

The torsion warping function F_ϕ in Eq. (17) is similar to the one used by Rehfield,[19] except that the variation of A_{ss} along the contour is taken into account in the present definition. The notation used for F_y, F_z, F_ϕ, S_y^*, and S_z^* is identical to the one used by Gjelsvik,[3] except for the term $[A_{nn} - (A_{ns}^2/A_{ss})]$ for composite construction. Gjelsvik derived these quantities by a flexibility approach and these are associated with the reactive or secondary shear flows. Analogous terms have also been derived by Mansfield[17] and Libove.[18] The warping functions in Eq. (17) account partially for the influence of A_{ns}; the influence of this term will be included later.

The displacement field for u given by Eq. (22) contains different levels of approximation. Ignoring $a_3(s)$, $a_4(s)$, and $a_5(s)$ and setting $\beta_z = -V_{,x}$ and $\beta_y = -W_{,x}$, results in the Euler–Bernoulli model. Ignoring $a_4(s)$ and $a_5(s)$ results in the first-order shear deformation model (Timoshenko theory), which has been used by Rehfield.[19] Inclusion of $a_4(s)$ and $a_5(s)$ results in the higher-order shear deformation theory.

IV. Static Response of Thin Walled Beams

Using the Timoshenko model, the displacement field is given by [Eqs. (15) and (1)]

$$\begin{aligned} u &= u_1(x) + y\beta_z(x) + z\beta_y(x) - a_3(s)\phi_{,x}(x) \\ v &= V(x) - z\phi(x) \\ w &= W(x) + y\phi(x) \end{aligned} \tag{18}$$

This results in the axial and shear strain given by

$$\begin{aligned} \varepsilon_{xx} &= u_{1,x} + y\beta_{z,x} + z\beta_{y,x} - \alpha_1 a_3 \phi_{,xx} \\ \gamma_{xs} &= u_{1,s} + (\beta_z + V_{,x})y_{,s} + (\beta_y + W_{,x})z_{,s} \\ &\quad - \alpha_2(a_{3,s} + r)\phi_{,x} \end{aligned} \tag{19}$$

These are of the same form as the strains derived by Rehfield,[19] except for the two parameters (α_1 and α_2), which will be determined later. Following Rehfield,[19] the generalized strains and the generalized stress resultants can be expressed as

$$q = [u_{1,x} \quad (\beta_z + V_{,x}) \quad (\beta_y + W_{,x}) \quad \phi_{,x} \quad \beta_{y,x} \quad \phi_{,xx}]^T \tag{20}$$

$$F = [N \quad Q_y \quad Q_z \quad M_x \quad M_z \quad Q_w]^T \tag{21}$$

The beam stiffness matrix $[K]$ is defined such that

$$\{F\} = [K]\{q\} \tag{22}$$

This $[K]$ is a 7×7 symmetric matrix and has the same form as the one derived by Rehfield,[19] with the difference that the constants α_1 and α_2 will be present in some of the elements. These two constants can be determined by imposing the condition that the strain energy of the internal forces is a minimum, i.e.,

$$\frac{\partial \bar{U}}{\partial \alpha_1} = 0, \qquad \frac{\partial \bar{U}}{\partial \alpha_2} = 0 \tag{23}$$

This results in a pair of simultaneous equations for α_1 and α_2 in terms of the sectional properties and the generalized strains q. This procedure is illustrated with reference to specific cases in the following sections.

V. Application to Thin-Walled Beams of Rectangular Cross Section

Composite thin-walled beams exhibit a number of couplings. Two specific types of construction are examined.

The first is the symmetrical or mirrorwise lay-up in which the value of A_{ns} is the same on both sides of the axis of symmetry, but has opposite signs. For this lay-up (with the axis of symmetry as the y axis), the nonzero elements of K are K_{11}, K_{12}, K_{22}, K_{33}, K_{44}, K_{45}, K_{55}, K_{66}, and K_{77}. This results in a coupling between the axial and shear deformations and between bending and twisting.

The second type of lay-up is the antisymmetric lay-up. If the axis of symmetry is the y axis, the nonzero elements of K are K_{11}, K_{14}, K_{22}, K_{25}, K_{33}, K_{36}, K_{44}, K_{55}, K_{66}, and K_{77}. The coupling is between the axial and torsional deformations and between bending and shear deformations.

For rectangular beams with symmetrical layup, Eq. (23) results in

$$\alpha_1 = 0$$

$$\alpha_2 = -\frac{\left(\oint A_{ss} r a_{3,s}\, ds\right)}{\left(\oint A_{ss} a_{3,s}^2\, ds\right)} - \left[\frac{\left(\oint A_{ns}\, z a_{3,s}^2\, ds\right)}{\left(\oint A_{ss} a_{3,s}^2\, ds\right)}\right]\left(\frac{\beta_{y,x}}{\phi_{,x}}\right) \tag{24}$$

This implies that the term $\phi_{,xx}$ is not present in ε_{xx}. The parameter α_2 consists of a constant part and a part that brings out the coupling between bending and torsion through the coupling term A_{ns}. The stiffness matrix (for the bending and torsional deformations) is

$$\begin{Bmatrix} M_x \\ M_y \end{Bmatrix} = \begin{bmatrix} K_{44} & K_{45} \\ K_{45} & K_{55} \end{bmatrix} \begin{Bmatrix} \phi_{,x} \\ \beta_{y,x} \end{Bmatrix} \tag{25}$$

where

$$\begin{aligned} K_{44} &= 4A^2 \Big/ \oint \left[\frac{ds}{A_{ss}}\right] \\ K_{45} &= 2A \oint \left[\frac{A_{ns}}{A_{ss}}\right] z\, ds \Big/ \oint \left[\frac{ds}{A_{ss}}\right] \\ K_{55} &= \oint A_{nn} z^2\, ds - \frac{\left[\oint A_{ns} z a_{3,s}\, ds\right]^2}{\oint A_{ss} a_{3,s}^2\, ds} \end{aligned} \tag{26}$$

For beams with constant A_{ss} along the contour, K_{44} and K_{45} are the same as those derived by Rehfield.[19] The bending stiffness K_{55} is lower than that derived by Rehfield because of the additional flexibility introduced by the coupling term A_{ns}. For the present case, Mansfield's method[17] gives the same values for K_{45} and K_{55}, but the bending stiffness is given by

$$K_{55}\,(\text{Mansfield} = \oint \left\{A_{nn} - \frac{A_{ns}^2}{A_{ss}}\right\} z^2\, ds + \frac{\left[\oint \left(\frac{A_{ns}}{A_{ss}}\right) z\, ds\right]^2}{\oint \left(\frac{ds}{A_{ss}}\right)} \tag{27}$$

For the beams considered in this article, Eqs. (26) and (27) give very close values.

For a beam of rectangular cross section, it is possible to express $a_3(s)$ as

$$a_3 = \beta yz \tag{28}$$

where

$$\beta = (\alpha - 1)/(\alpha + 1) \tag{29}$$

$$\alpha = b/a \quad \text{(Rehfield[19])}$$

$$\alpha = bG^F_{\text{eff}}/aG^W_{\text{eff}} \quad \text{(Smith and Chopra[22])} \tag{30}$$

$$\alpha = bA^F_{ss}/aA^W_{ss} \quad \text{(Present article)}$$

For beams having no variation in the effective shear modulus (G_{eff} or A_{ss}) along s, all of the previous definitions give the same values for α.

Figures 1–6 show the bending slope and the twist caused from unit tip load for the beams tested by Chandra et al.[27] at the University of Maryland. These beams had the following dimensions: length, 30 in.; flange width, 0.953 in.; and web height, 0.597 in. The walls were 0.032 in. thick, the lay-up of the flanges was $(\theta)_6$, and that of the webs was $(\theta/-\theta)_3$. Beams S2, S3, and S4 had values of θ = 15, 30, and 45 deg, respectively. Figures 1–6 display the following results: 1) experimental values[27] (denoted by E), 2) finite element analysis of Stemple and Lee[9] (denoted by F), 3) Smith and Chopra method[22] (denoted by S-C), 4) Mansfield's method[17] (denoted by M), 5) Rehfield's method with $\alpha = b/a$ (denoted by R1), 6) Rehfield's method with $\alpha = bA^F_{ss}/aA^W_{ss}$ and with K_{55} as given by Rehfield (denoted by R2), and 7) the present method (denoted by R3). The first three of the previous results are taken from Ref. 22.

The results from the present method (R3) and those from Mansfield's method (M) are almost identical and are close to the FEM of Stemple and Lee,[9] who used a beam finite element with the cross section warpings determined by a FEM.

Considering first the bending slope from the unit tip load, Rehfield's method underestimates the response since it does not account for the additional flexibility because of the A_{ns} term. The results from the FEM, M, and R3 are close to each other. As fiber orientation increases from 15 to 45 deg, the method of Smith and Chopra gives better correlations with

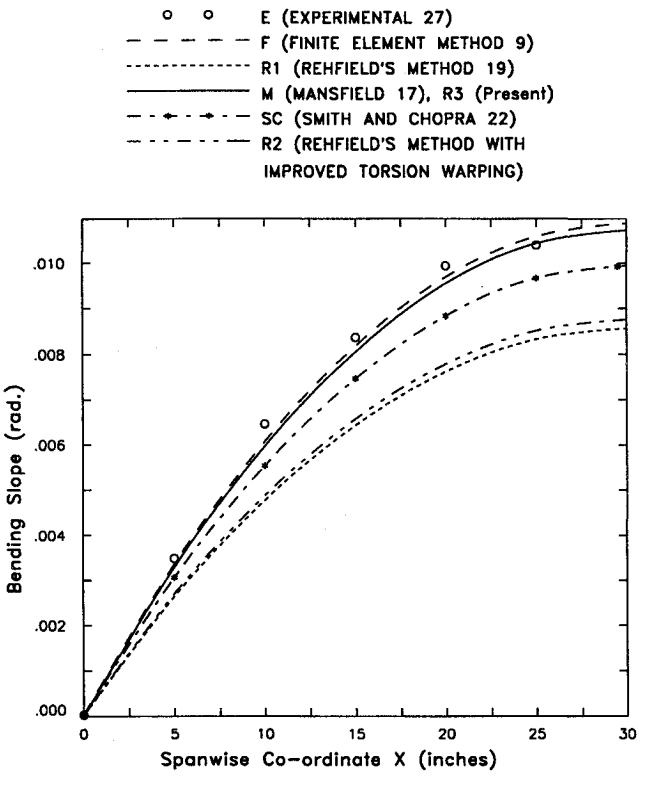

Fig. 1 Bending slope caused by the unit tip load, bending–torsion coupled graphite epoxy (15 deg).

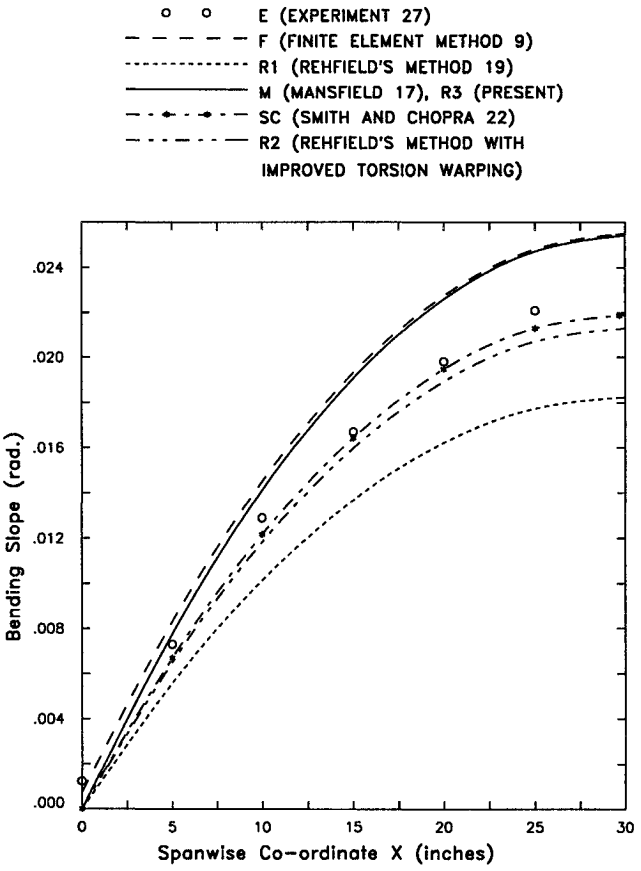

Fig. 2 Bending slope caused by the unit tip load, bending–torsion coupled graphite epoxy (30 deg).

experimental results than the other methods. The results for the twist under tip load show that the FEM, M, and R3 give better correlations than the other methods.

These results show that accurate results can be obtained by the Euler–Bernoulli model provided the torsion-related warping and the additional bending flexibility caused by the coupling term A_{ns} are properly represented.

VI. Vibrations of a Composite Beam of Solid Rectangular Cross Section

Reference 30 presents the experimental results for composite beams of rectangular cross section. The beams were 0.5 in. wide and 0.125 in. thick with a double cantilever length of 15 in. Graphite fiber and boron fiber beams with lay-ups of 0, 15, 30, and 90 deg were tested. Reference 30 also contains theoretical results.

The 15- and 30-deg beams exhibit coupling between bending and torsion. With b and h representing width and depth of the beam, the bending, torsion, and coupling stiffnesses are given by the present method as

$$K_{55} = \bar{Q}_{11}I_y\left[1 - \frac{\bar{Q}^2_{16}}{\bar{Q}^2_{11}\{\bar{Q}_{66}/\bar{Q}_{11} + \bar{Q}_{44}h^2/\bar{Q}_{11}b^2\}}\right]$$

$$K_{44} = 4\bar{Q}_{66}I_y/\{1 + \bar{Q}_{66}h^2/\bar{Q}_{11}b^2\} \tag{31}$$

$$K_{45} = 2\bar{Q}_{16}I_y/\{1 + \bar{Q}_{66}h^2/\bar{Q}_{11}b^2\}$$

The corresponding stiffnesses obtained by a flexibility method[31] are

$$K_{55} = \bar{Q}_{11}I_y[1 - 0.63(a\bar{Q}^2_{16}/b\bar{Q}_{11})]$$

$$K_{44} = 4\bar{Q}_{66}I_y[1 - 0.63a/b] \tag{32}$$

$$K_{45} = 2\bar{Q}_{16}I_y[1 - 0.63a/b]$$

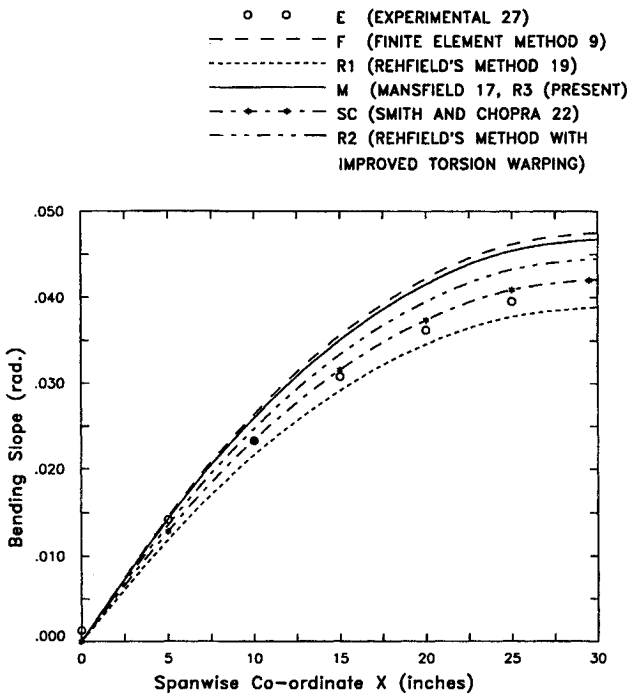

Fig. 3 Bending slope caused by the unit tip load, bending–torsion coupled graphite epoxy (45 deg).

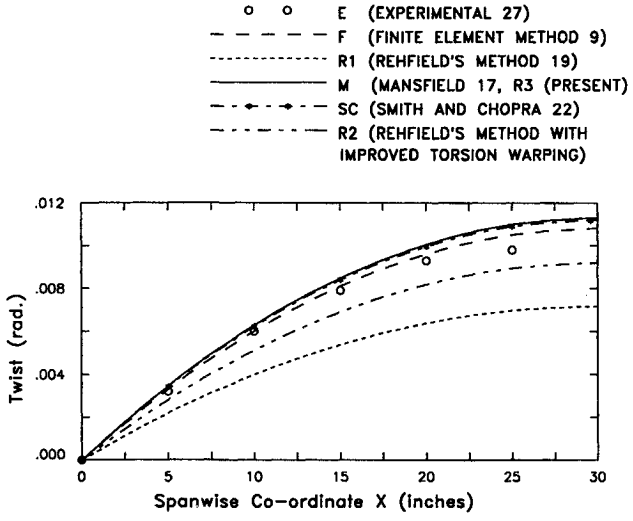

Fig. 4 Twist caused by the unit tip load, bending–torsion coupled graphite epoxy (15 deg).

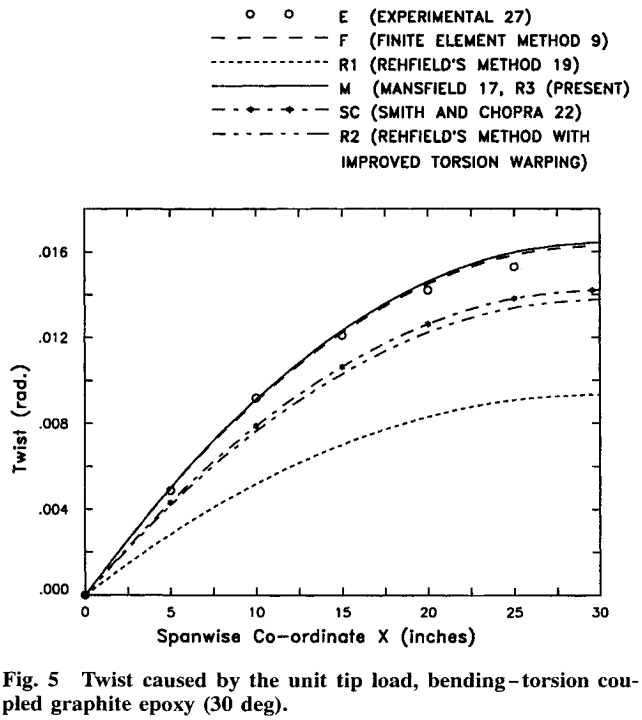

Fig. 5 Twist caused by the unit tip load, bending–torsion coupled graphite epoxy (30 deg).

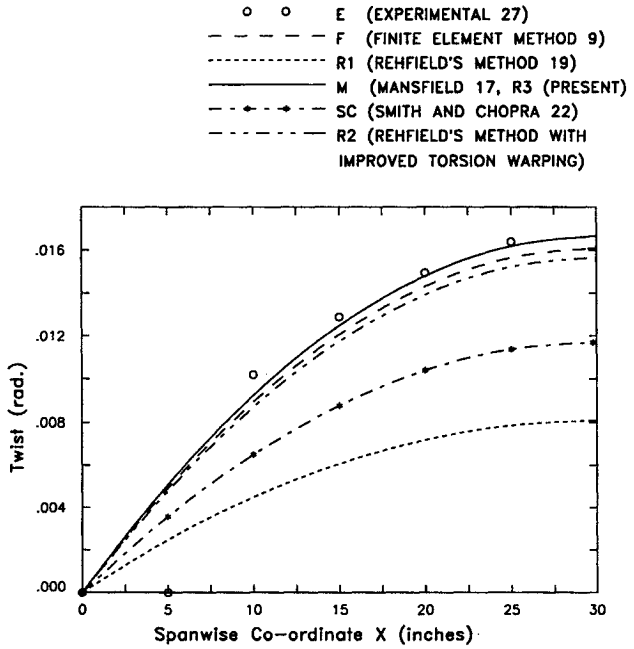

Fig. 6 Twist caused by the unit tip load, bending–torsion coupled graphite epoxy (45 deg).

As in the case of the thin-walled beam, the reduction in bending stiffness because of the coupling term Q_{16} (similar to A_{ns}) is brought out by both methods.

Tables 1 and 2 give the correlations of the results obtained by the present method with experimental results and also with those obtained by other investigators. Tables 1 and 2 contain the following results for the 15- and 30-deg beams: 1) model R1 with the torsion related warping ignored, 2) model R1 with inclusion of torsion related warping (model R1BT), 3) model R1BT with shear deformation included (model R1BST), 4) present method with shear deformation neglected (model R3BT), 5) theoretical results from Abarcar and Cunniff[30] based on the flexibility approach, 6) theoretical results from a flexibility approach following Suresh and Venkatesan[31] (model BST), 7) theoretical results from Mukherjee[32] who used a stiffness approach including higher-order shear deformation theory combined with the FEM, 8) theoretical results from Hodges et al.[33] who used a model similar to R1BST, 9) results from Kapania and Raciti[34] who used a model similar to model S-C by using a modified constitutive relation, and 10) experimental results from Abarcar and Cunniff.[30]

All of the beams exhibit a number of couplings. However, in the following discussion, the modes that are predominantly bending or predominantly torsion will be referred to as bending and torsion modes, respectively.

An examination of Tables 1 and 2 reveals the following:

1) The neglect of torsion related warping grossly overestimates the bending and torsion frequencies (between 29–45% in the case of boron–epoxy and between 21–37% for graphite–epoxy beams).

2) Inclusion of the torsion-related warping (model R1BT),

Table 1 Frequencies of graphite-epoxy beam

Sl no.	R1	R1BT	R1BST	Present	BST	Hodges et al.[33]	Abarcar and Cunniff[30]	Mukherjee[32]	Abarcar and Cuniff experiment[30]
					a) 15-deg beam				
1	109.9	85.4	85.3	82.16	85.4	77.35	84.0	82.5	82.5
2	687.5	532.0	529.1	511.4	532.0	479.19	521.4	517.9	511.3
3	1757.7	1472.2	1454.4	1411.1	1468.7	1317.3	1430.3	1437.4	1423.4
4	1923.3	1768.7	1769.3	1588.6	1627.7	1476.0	1604.0	1562.6	1526.9[a]
5	3751.8	2859.5	2798.9	2742.3	2857.6	——	2754.8	2784.9	2783.6
6	5282.8	4573.6	4515.6	4368.4	4524.7	——	4352.5	4535.6	4364.6
7	6129.6	5369.4	5532.3	4834.2	5010.0	4517.2	4853.5	4693.2	4731.6[a]

Sl no.	R1	R1BT	R1BST	Present	BST	Kapania and Raciti[34]	Hodges et al.[33]	Abarcar and Cunniff[30]	Mukherjee[32]	Abarcar and Cuniff experiment[30]
						b) 30-deg beam				
1	72.5	52.6	52.6	52.6	52.6	52.65	48.97	52.7	53.1	52.7
2	453.8	329.1	328.2	329.1	329.1	329.78	307.85	329.3	330.5	331.8
3	1269.5	918.1	912.6	918.0	918.0	928.29	869.06	915.9	921.6	924.7
4	2041.4	1785.0	1766.4	1745.7	1777.3	——	1660.9	1767.0	1781.0	1766.9
5	2485.0	2051.7	2058.2	1818.9	1891.6	1818.42	——	1896.5	1798.3	1827.4[a]
6	4110.4	2948.4	2865.9	2922.1	2929.9	——	——	2901.4	2956.3	2984.0
7	5948.1	4474.6	4190.1	4211.9	4299.7	——	5056.1	4263.9	4398.2	4432.4

[a]Indicates predominantly torsional mode.

Table 2 Frequencies of boron-epoxy beam

Sl no.	R1	R1BT	R1BST	Present	BST	Abarcar and Cunniff[30]	Mukherjee[32]	Abarcar and Cuniff experiment[30]
					a) 15-deg beam			
1	132.3	96.82	96.7	96.8	96.8	91.1	91.1	91.0
2	827.8	602.6	598.4	602.5	602.5	563.7	565.8	567.2
3	2130.58	1666.2	1640.3	1661.4	1663.96	1543.4	1567.7	1575.5
4	2315.8	2142.6	2142.7	1870.1	1971.2	1865.3	1721.7	1767.4[a]
5	4509.9	3231.4	3145.3	3227.1	3229.0	2958.4	3029.9	3073.6
6	6380.4	5155.0	5006.9	5157.7	5179.6	4681.1	4922.8	4926.7
					b) 30-deg beam			
1	89.2	64.96	64.9	62.58	64.96	62.5	62.5	62.5
2	559.0	406.3	405.1	391.4	406.3	390.1	390.2	391.7
3	1563.98	1134.1	1126.4	1092.6	1134.1	1084.6	1088.8	1090.5
4	2717.7	2209.7	2182.7	2121.4	2206.6	2097.5	2125.5	2107.7
5	3062.9	2720.5	2707.4	2280.1	2503.6	2343.1	2248.1	2174.3[a]
6	5056.6	3639.6	3572.8	3480.1	3675.5	3433.4	3502.3	3542.4

[a]Indicates predominantly torsional mode.

vastly improves the correlations even without the inclusion of shear deformation.

3) Model R1BST gives more marginally improved correlations than model R1BT.

4) The present method, even without the inclusion of transverse shear deformation (R3BT), gives much better correlations than the previous models since it includes the reduction in the effective bending stiffness caused by Q_{16}. The correlations are especially good for the torsional frequencies.

5) The results from the present method are close to the values obtained by using a flexibility approach[31] where the stiffnesses are obtained through Lekhnitskii's[35] elasticity solution.

6) The results from the theory of Abarcar and Cunniff,[30] which is based on the flexibility approach, give good correlations with experiment.

7) The best correlations are obtained by Mukherjee[32] who includes the influence of higher-order shear deformation.

8) Although the results of Hodges et al.[33] may be expected to be close to the R1BST model, it is puzzling to note the poorer correlations. Their results underestimate the frequencies. Also, they do not obtain all of the frequencies obtained by the others, even though they obtain some additional frequencies not reported by others.

9) The results of Kapania and Raciti[34] are close to those obtained by model R1BST.

These comparisons show that for these beams, which exhibit strong couplings especially between bending and torsion, it is possible to predict the frequencies accurately in the Euler–Bernoulli framework provided that the torsion-related warping is optimized as done in the present method.

VII. Results from the Higher-Order Shear Deformation Theory

The higher-order shear deformation theory will first be validated against a mixed variational formulation for isotropic beams,[29] where a cantilever thin-walled beam of rectangular cross section of width b to depth h ratio of 2 and subjected to a concentrated load P at the free end was considered as an example. The tip deflection by the present theory is given by

$$W = (PL^3/3K_{55})[1 + 10.457\alpha^2 - 2.2799\alpha^3 \tanh(\lambda L)] \quad (33)$$

For the same beam, Timoshenko's theory gives the tip deflection as

$$W = (PL^3/3K_{55})[1 + 2.333\alpha^2/K] \tag{34}$$

In Eqs. (33) and (34)

$$K_{55} = \text{bending rigidity}$$
$$\alpha^2 = (b/L)^2(A_{nn}/A_{ss})$$
$$\lambda = 1.521/\alpha \tag{35}$$

K = Timoshenko shear coefficient, which depends upon A_{nn} and A_{ns} (Ref. 28)

The present theory [Eq. (33)] does not need the assumption of a shear coefficient. The variable α is a modified slenderness ratio, which is a similarity parameter, and λ is a decay parameter. The nondimensional static response of different beams will be similar if they have the same value of α.

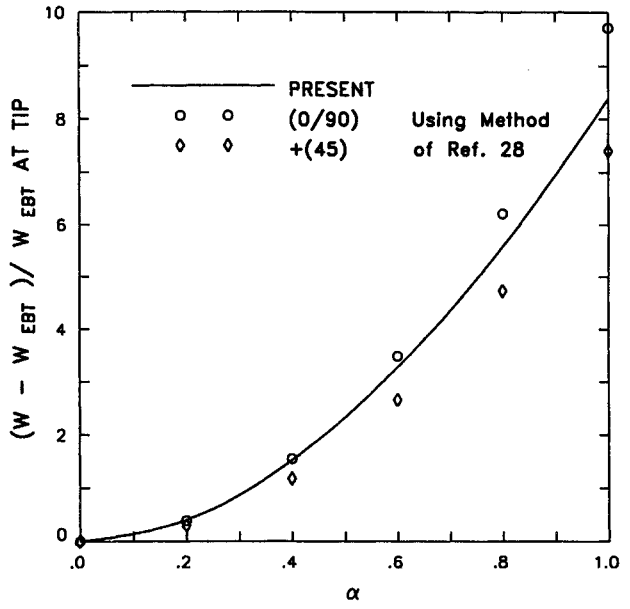

Fig. 7 $(W - W_{EBT})/W_{EBT}$ for thin-walled beam of rectangular cross section as a function of modified slenderness ratio $a = \sqrt{A_{ns}/A_{ss}}$.

If we denote the deflection according to the Euler–Bernoulli theory by W_{EBT}, the parameter $(W - W_{EBT})/W_{EBT}$ represents the nondimensional change in the tip deflection caused by shear effects. The variation of this parameter as a function of α is shown in Fig. 7. Low values of α represent either low values of b/L (long, slender beams) or low values of Young's modulus to shear modulus ratio. Figure 7 shows that for values of α greater than about 0.4, shear deformations become important and the Euler–Bernoulli theory can grossly underestimate the deflections. The present theory gives a single curve for different types of lay-ups, whereas Timoshenko's theory, with K calculated from Banks' method[28] gives values depending upon the ratio of (A_{nn}/A_{ss}).

Figure 8 shows the distribution of the nondimensional axial stress at the fixed end for a beam whose walls are made of isotropic material. Also shown are the corresponding values obtained from the Euler–Bernoulli theory and by the method of Koo and Cheung,[29] who used a mixed variational formulation for obtaining both the displacements and stresses including shear lag effects for isotropic beams. The warping functions used by them are very similar to the ones used in this article. The present method using a single warping mode shows excellent agreement with the results obtained by Koo and Cheung using two and three warping functions.

For a thin-walled beam ($a = 2b$) with walls made of carbon fiber, Fig. 9 shows the distribution of the nondimensional axial stress at the root for (0/90-deg) and (±45-deg) lay-ups. Also shown are the corresponding values for an isotropic beam and the values from the Euler–Bernoulli theory. [The values for beam with (±30-deg) lay-up, which has not been shown in the figure, are very close to the isotropic beam values.] The importance of (A_{nn}/A_{ss}) is clearly seen with the shear lag effects being predominant in the beam with (0/90-deg) layup and being lower than the isotropic beam values for the (±45-deg) lay-up.

Figure 10 shows the spanwise distribution of the nondimensional axial stress at one corner of the beam. For the beam with (0/90-deg) lay-up, the shear lag effects persist almost over the entire span, whereas for the (±45-deg) lay-up, they decay very rapidly. For the (±45-deg) lay-up, the value at 20% of the span is just 4.5% above the value predicted by the Euler–Bernoulli theory.

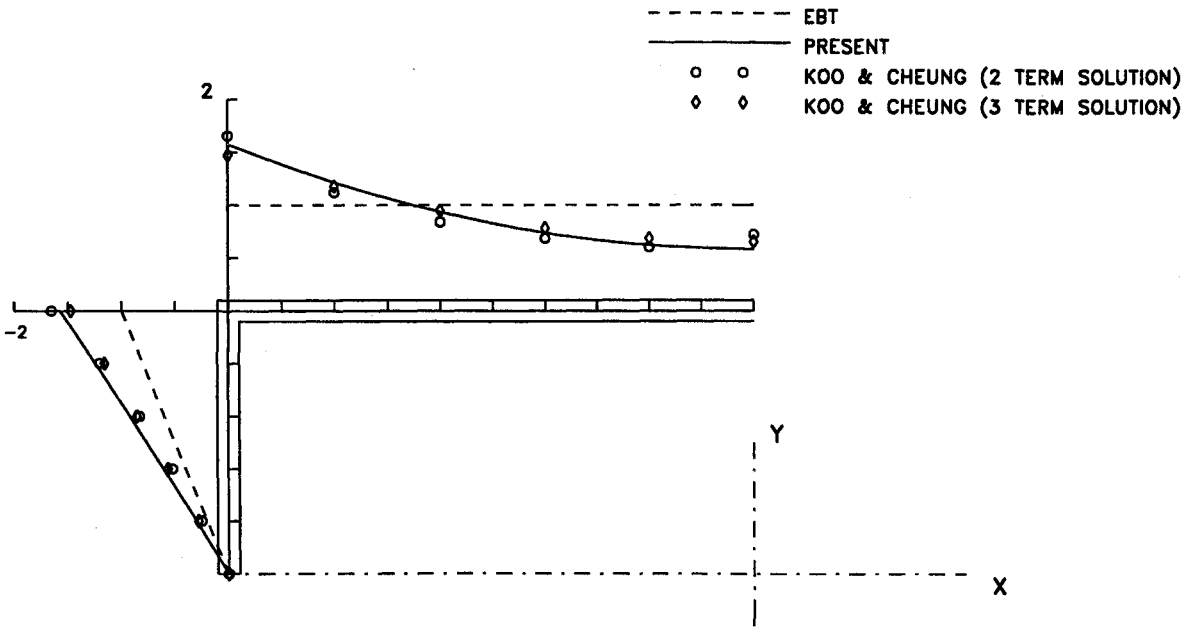

Fig. 8 Nondimensional axial stress at fixed end of thin-walled rectangular beam.

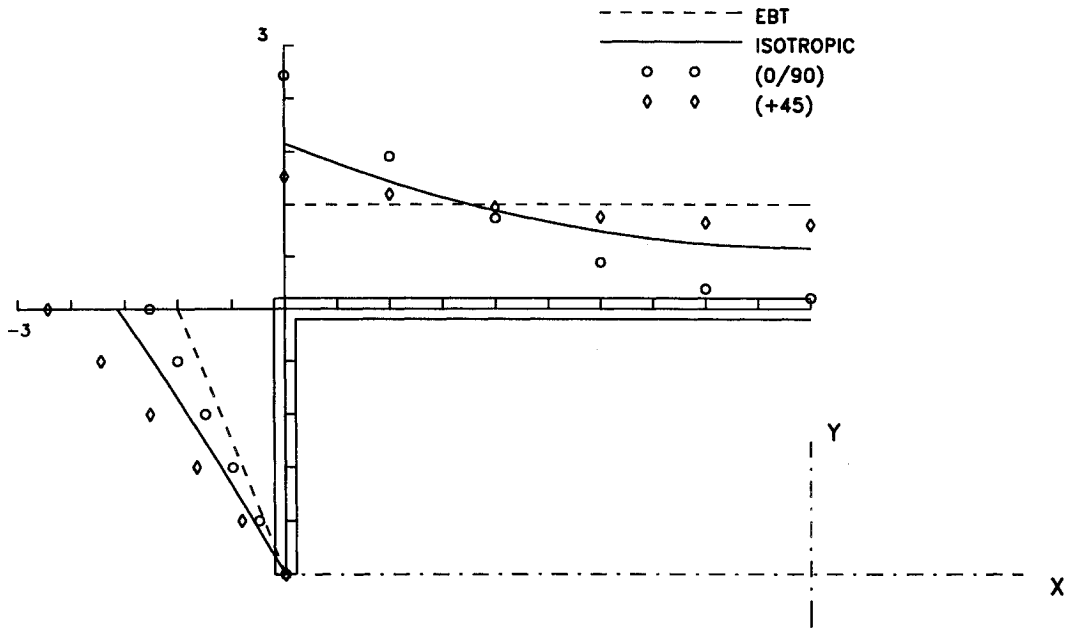

Fig. 9 Nondimensional axial stress at fixed end of thin-walled beam of rectangular cross section.

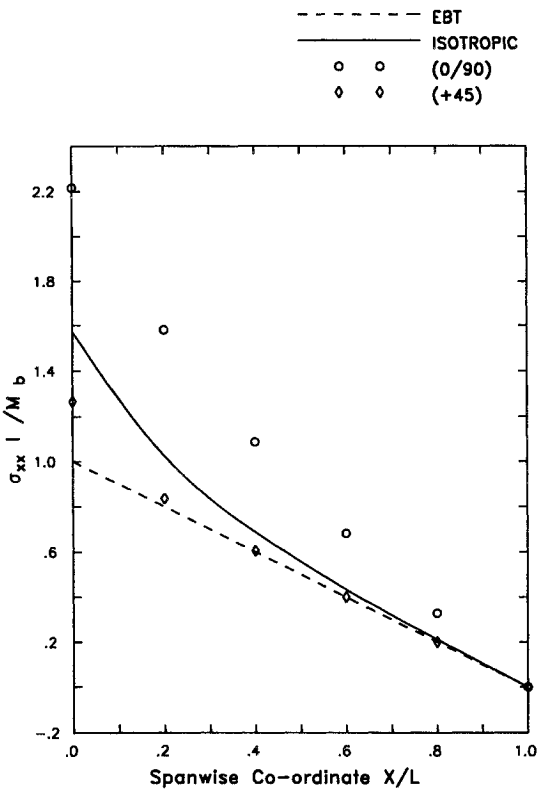

Fig. 10 Spanwise distribution of axial stress at corner of cantilever beam with tip load ($z = 1$ and $y = 1$).

As an additional validation of the present theory, the cantilever beam ($b = 4h$) subject to a uniformly distributed load analyzed by Bauchau[12] is considered. For this beam, tip deflection $(W_{TIP}/fL^4) \times 10^{-6}$ was 4.66 m. The corresponding values obtained by Bauchau[12] are 4.604 and 4.677 m by the Bernoulli and St-Venant methods using four eigenwarping terms. The tip–twist under distributed torque $(\theta_{TIP}/m_0L^4) \times 10^{-6}$ for this beam is 129.1 by the present method compared with 126.7 (Bernoulli) and 130.0 (St-Venant) methods obtained by Bauchau[12] using four eigenwarping terms. The correlation between the two methods is good.

VIII. Comparison with Other Theories

The objective of a beam theory is to reduce a three-dimensional problem to a one-dimensional problem by separating the three-dimensional state of stress into section properties and other quantities like deflections that depend upon the lengthwise coordinate. Various levels of approximations start with the Euler–Bernoulli model with its well-known assumptions. The next level of approximation is the Timoshenko model that considers the influence of transverse shear deformations and introduces a shear correction factor to account for the parabolic variation of shear stress across the cross section. Higher-order shear deformation theories consider the influence of additional cross-sectional deformations (warpings). As shown in the examples considered in this article, these warpings can have a significant effect on the deflections, frequencies, and stresses, depending on the beam geometry and material characteristics.

For beams of general cross section, an important ingredient is the choice of warping function. References 8–10 are representative examples of the use of FEMs for the determination of the warping functions. Bauchau[12] uses the concept of eigenwarpings.

The present theory differs from the earlier theories in two respects:

1) The warping functions are derived from a consideration of the equilibrium equations for an equivalent isotropic cross section, and taking into account the variation of $(A_{nn} - A_{ns}^2/A_{ss})$ and A_{ss} along the contour. This enables the use of the well-established warping functions of isotropic structures as trial functions in the analysis.

2) The influence of A_{ns} is taken into account by the introduction of the factors α_1 and α_2 and by minimizing the strain energy density with respect to α_1 and α_2. As was shown for both thin-walled and solid cross-sectional beams, this brings out the couplings, and for symmetric lay-ups, correctly accounts for the reduction in bending stiffness. These improve Rehfield's theory and are responsible for the close agreement between the present theory and Mansfield's theory.

IX. Concluding Remarks

This article has attempted a simple framework for the theoretical analysis of thin-walled composite beams. By comparison with experimental results for both static and vibration responses, the importance of adequate modeling of the torsion-related warping has been brought out. By optimizing the tor-

sion- and shear-related warping so that their contribution to the strain–energy is minimum, the effect of reduction in the effective bending stiffness of symmetrically laminated constructions is derived. The results for both static and vibration responses show that the Euler–Bernoulli model can give very accurate results when the torsion-related warping is adequately modeled.

For obtaining good correlations for stresses, it is necessary to use the higher-order shear deformation theory. The present higher-order theory has been validated against results from other theoretical methods for both deflections and stresses. For beams of rectangular cross section, a modified slenderness ratio has been derived as a similarity parameter for comparing the responses of different beams. For certain beams, it is possible for the shear-lag effects to persist over the entire length of the beam.

References

[1]Czerwenka, G., and Schnell, W., "Einfuhrung in Die Rechenmethodenden Des Leichtbaus," Bibliographiches Inst., Mannheim, Germany, 1967, Chap. 4.

[2]Murray, N. W., *Introduction to the Theory of Thin-walled Structures*, Clarendon, Oxford, England, UK, 1986, pp. 54–134, Chap. 2.

[3]Gjelsvik, A., *The Theory of Thin Walled Beams*, Wiley, New York, 1981, pp. 100–115.

[4]Schade, D., "Eine Eindimensionale Darstellung der Torsion and Profilverformung von Dunnwandige, Prismatischen Staben," *Ingenieur-Archiv*, Vol. 57, No. 6, 1987, pp. 420–430.

[5]Krishna Murty, A. V., "Towards a Consistent Beam Theory," *AIAA Journal*, Vol. 22, No. 6, 1984, pp. 811–816.

[6]Krishna Murty, A. V., "Analysis of Short Beams," *AIAA Journal*, Vol. 8, No. 11, 1970, pp. 2098–2100.

[7]Krishna Murty, A. V., "General Theory of Vibration of Cylindrical Tubes: Part I," *Journal of Aeronautical Society of India*, Vol. 20, No. 1, 1968, pp. 1–38.

[8]Worndle, R., "Calculation of the Cross Section Properties and the Shear Stresses of Composite Rotor Blades," *Vertica*, Vol. 6, No. 2, 1982, pp. 111–129.

[9]Stemple, A. D., and Lee, S. W., "Finite Element Modeling for Composite Beams with Arbitrary Cross Sectional Warping," *AIAA Journal*, Vol. 16, No. 12, 1988, pp. 1512–1520.

[10]Kosmatka, J. B., and Friedmann, P. P., "Vibration Analysis of Composite Turbo Propellers Using a Non-Linear Beam Type Finite-Element Approach," *AIAA Journal*, Vol. 27, No. 11, 1989, pp. 1606–1614.

[11]Bauchau, O. A., Coffenberry, B. S., and Rehfield, L. W., "Composite Box Beam Analysis: Theory and Experiments," *Journal of Reinforced Plastics and Composites*, Vol. 6, No. 1, 1987, pp. 25–35.

[12]Bauchau, O. A., "A Beam Theory for Anisotropic Materials," *Journal of Applied Mechanics*, Vol. 52, No. 2, 1985, pp. 416–422.

[13]Bauchau, O. A., and Hong, C. H., "Large Displacement Analysis of Naturally Curved and Twisted Composite Beams," *AIAA Journal*, Vol. 25, No. 10, 1987, pp. 1469–1475.

[14]Bauchau, O. A., and Hong, C. H., "Non-Linear Composite Beam Theory," *Journal of Applied Mechanics*, Vol. 55, No. 1, 1988, pp. 156–163.

[15]Kosmatka, J. B., "Extension, Bending and Torsion of Anisotropic Beams with Initial Twist," *Proceedings of the AIAA/ASME/ASCE/AHS/ASC 30th Structures, Structural Dynamics, and Materials Conference*, AIAA, Washington, DC, 1989, pp. 1799–1806.

[16]Kosmatka, J. B., "Analysis of Composite Rotor Blades via St. Venant's Elasticity Solutions," 14th European Rotorcraft Forum, Sept., 1988.

[17]Mansfield, E. H., and Sobey, A. J., "The Fibre Composite Helicopter Blade—Part I: Stiffness Properties; Part II: Prospects for Aeroelastic Tailoring," *Aeronautical Quarterly*, Vol. 30, No. 2, 1979, pp. 413–449.

[18]Libove, C., "Stresses and Rate of Twist in Single Cell Thin-Walled Beams with Anisotropic Walls," *AIAA Journal*, Vol. 26, No. 9, 1988, pp. 1107–1117.

[19]Rehfield, L. W., "Design Analysis Methodology for Composite Rotor Blades," DOD/NASA Conf. on Fibre Composites in Structural Design, Denver, CO, June 1985.

[20]Nixon, M. W., "Extension-Twist Coupling of Composite Circular Tubes and Application to Tilt Rotor Blade Design," *Proceedings of the AIAA 28th Structures, Structural Dynamics, and Materials Conference*, AIAA, New York, 1987, pp. 295–303.

[21]Rehfield, L. W., Atilgan, A. R., and Hodges, D. H., "Nonclassical Behaviour of Thin-Walled Composite Beams with Closed Cross-Sections," *Journal of the American Helicopter Society*, Vol. 35, No. 2, 1990, pp. 42–50.

[22]Smith, E. C., and Chopra, I., "Formulation and Evaluation of an Analytical Model for Composite Box Beams," *Journal of the American Helicopter Society*, Vol. 36, No. 3, 1991, pp. 23–35.

[23]Rand, O., "Periodic Response of Thin-walled Composite Blades," *45th Annual Forum of the American Helicopter Society* (Boston, MA), 1989, pp. 1017–1029.

[24]Rand, O., "Theoretical Modelling of Composite Rotating Beams," *Vertica*, Vol. 14, No. 3, 1990, pp. 329–343.

[25]Chandra, R., and Chopra, I., "Structural Dynamics of Two-Cell Composite Rotor Blades with Elastic Couplings," *AIAA Journal*, Vol. 30, No. 12, 1992, pp. 2914–2921.

[26]Hodges, D. H., "Review of Composite Rotor Blade Modelling," *AIAA Journal*, Vol. 28, No. 3, 1990, pp. 561–565.

[27]Chandra, R., Stemple, A. D., and Chopra, I., "Thin Walled Composite Beams Under Bending, Torsional and Extensional Loads," *Journal of Aircraft*, Vol. 27, No. 7, 1990, pp. 619–627.

[28]Banks, L. C., "Shear Coefficients for Thin-Walled Composite Beams," *Composite Structures*, Vol. 8, No. 1, 1987, pp. 47–61.

[29]Koo, K. K., and Cheung, Y. K., "Mixed Variational Formulation for Thin-Walled Beams with Shear Lag," *Journal of Engineering Mechanics*, Vol. 115, No. 10, 1989, pp. 2271–2286.

[30]Abarcar, R. B., and Cunniff, P. F., "The Vibration of Cantilever Beams of Fiber Reinforced Material," *Journal of Composite Materials*, Vol. 6, No. 4, 1972, pp. 504–517.

[31]Suresh, J. K., Venkatesan, C., and Ramamurti, V., "Structural Dynamic Analysis of Composite Beams," *Journal of Sound and Vibration*, Vol. 143, No. 3, 1990, pp. 503–519.

[32]Mukherjee, A., "Free Vibration of Laminated Beams and Stiffened Plates Using a Higher-Order Element," *Aeronautical Journal of the Royal Aeronautical Society*, April 1991, pp. 124–131.

[33]Hodges, D. H., Atilgan, A. R., Fulton, M. V., and Rehfield, L. W., "Free Vibration Analysis of Composite Beams," *Journal of the American Helicopter Society*, Vol. 36, No. 3, 1991, pp. 36–47.

[34]Kapania, R. K., and Raciti, S., "Nonlinear Vibrations of Unsymmetrically Laminated Beams," *AIAA Journal*, Vol. 27, No. 2, 1989, pp. 201–219.

[35]Lekhnitskii, S. G., *Theory of Elasticity of an Anisotropic Body*, Mir Publishers, Moscow, Russia, 1981.